

# Serine Metabolism Controls Dental Pulp Stem Cell Aging by Regulating the DNA Methylation of p16

Journal of Dental Research  
2021, Vol. 100(1) 90–97  
© International & American Associations  
for Dental Research 2020  
Article reuse guidelines:  
sagepub.com/journals-permissions  
DOI: 10.1177/0022034520958374  
journals.sagepub.com/home/jdr

R.L. Yang<sup>1,2,3</sup>, H.M. Huang<sup>1,2,3</sup>, C.S. Han<sup>1,2,3</sup>, S.J. Cui<sup>1,2,3</sup>, Y.K. Zhou<sup>1,2,3</sup>,  
and Y.H. Zhou<sup>1,2,3</sup>

## Abstract

To investigate the characteristics and molecular events of dental pulp stem cells (DPSCs) for tissue regeneration with aging, we isolated and analyzed the stem cells from human exfoliated deciduous teeth (SHED) and permanent teeth of young (Y-DPSCs) and old (A-DPSCs) adults. Results showed that the stemness and osteogenic differentiation capacity of DPSCs decreased with aging. The RNA sequencing results showed that glycine, serine, and threonine metabolism was one of the most enriched gene clusters among SHED, Y-DPSCs, and A-DPSCs, according to analysis based on the Kyoto Encyclopedia of Genes and Genomes. The expression of serine metabolism-related enzymes phosphoserine aminotransferase 1 (PSAT1) and phosphoglycerate (PHGDH) decreased in A-DPSCs and provided less methyl donor S-adenosylmethionine (SAM) for DNA methylation, leading to the hypomethylation of the senescence marker p16 (CDNK2A). Furthermore, the proliferation and differentiation capacity of Y-DPSCs and SHED decreased after PHGDH siRNA treatment, which reduced the level of SAM. Convincingly, the ratios of PSAT1-, PHGDH-, or proliferating cell nuclear antigen-positive cells in the dental pulp of old permanent teeth were less than those in the dental pulp of deciduous teeth and young permanent teeth. In summary, the stemness and differentiation capacity of DPSCs decreased with aging. The decreased serine metabolism in A-DPSCs upregulated the expression of p16 via attenuating its DNA methylation, resulting in DPSC aging. Our finding indicated that serine metabolism and 1 carbon unit participated in stem cell aging, which provided new direction for stem cell aging study and intervention.

**Keywords:** stemness, osteogenic differentiation, human exfoliated teeth, permanent teeth, mesenchymal stem cells, tissue regeneration

## Introduction

Dental pulp stem cells (DPSCs), a population of stem cells residing in the pulp, have been isolated from human deciduous teeth (SHED) and permanent teeth pulp. DPSCs and SHED possess a multilineage differentiation capacity, which can differentiate into odontogenic, osteogenic, adipogenic, and chondrogenic lineages (Gronthos et al. 2000; Miura et al. 2003). DPSCs and SHED, like bone marrow mesenchymal stem cells, show profound immunomodulation capacity (Yamaza et al. 2010). As an abundant resource and for the nontraumatic isolation of DPSCs, they can be involved in the regeneration of dentin structure or the repair of injured tooth and used for immune disease therapy (Tang et al. 2019). SHED, which are isolated from deciduous teeth, show superior proliferation and differentiation capacity than DPSCs and bone marrow mesenchymal stem cells (Xuan et al. 2018). The differentiation and proliferation capacities of mesenchymal stem cells isolated from older individuals' bone marrow and adipose tissue are decreased as compared with those from young individuals' bone marrow and adipose tissue (Alt et al. 2012; Liu et al. 2018). DPSCs similarly show an age-dependent decline in their regenerative capacity (Nozu et al. 2018). However, the characteristic alteration among SHED and DPSCs isolated from young (Y-DPSCs) and old (A-DPSCs) adults is not clear. The underlying molecular mechanism also needs further investigation.

Serine, a nonessential amino acid, is the substrate for NADPH production and nucleotide biosynthesis. The serine-related metabolic pathways form a complex network, called one-carbon metabolism (Locasale 2013; Yang and Vousden 2016). One-carbon metabolism is supported by the uptake of serine from the external microenvironment or de novo synthesis. Multiple serine pathway enzymes—including phosphoserine aminotransferase 1 (PSAT1), phosphoglycerate (PHGDH), phosphoserine phosphatase (PSPH), and hydroxymethyltransferases (SHMT) 1 and 2—participate in the de novo synthesis of serine. For instance, PHGDH converts phosphoglycerate into phosphohydroxypyruvate to generate serine, and the reversible reaction of serine to glycine is catalyzed by SHMT1

<sup>1</sup>Department of Orthodontics, Peking University, School and Hospital of Stomatology, Beijing, China

<sup>2</sup>National Clinical Research Center for Oral Diseases and National Engineering Laboratory for Digital and Material Technology of Stomatology, Beijing, China

<sup>3</sup>Beijing Key Laboratory of Digital Stomatology, Beijing, China

A supplemental appendix to this article is available online.

## Corresponding Author:

R.L. Yang, Department of Orthodontics, Peking University, School and Hospital of Stomatology, 22 Zhongguancun Avenue South, Haidian District, Beijing, 100081, China.  
Emails: ruiiliyangabc@163.com; ruiiliyang@bjmu.edu.cn

and SHMT2. Serine metabolism can also fuel the methionine salvage pathway, which is the main mechanism of synthesis of the methyl donor S-adenosyl methionine (SAM; Mentch et al. 2015; Maddocks et al. 2016). SAM is the universal donor of methyl groups to DNA and histone methyltransferases. DNA methyltransferase enzymes DNMT1, DNMT3a, and DNMT3b methylate the DNA base cytosine to 5-methylcytosine (5-mC), which is a major transcriptional repressive mark in a variety of eukaryotes (Etchegaray and Mostoslavsky 2016; Rodriguez et al. 2019; Kurniawan et al. 2020). Recent studies show that serine-dependent one-carbon metabolism regulates neural stem cell differentiation by altering the methylation of H3K4 (Fawal et al. 2018). One-carbon metabolism controls the fate of embryonic stem cells via epigenetic DNA and histone modifications (Van Winkle and Ryznar 2019). Studies report the indicators of aging, such as a reduction in proliferation, telomerase shortening, differentiation capacity, and morphologic abnormalities of cells (Sharpless and DePinho 2007; Ren et al. 2017; Morsczech 2019). However, whether serine-dependent one-carbon metabolism dictates the cell fate or function of DPSCs is unknown.

In this study, we have identified that serine metabolism is one of the most enriched gene clusters among SHED, Y-DPSCs, and A-DPSCs by using RNA sequencing analysis. Serine metabolism declines in DPSCs in an age-dependent manner, and this decline is accompanied by decreased stem cell proliferation and osteogenic differentiation. Furthermore, decreased serine metabolism reduces the methyl donor SAM, which leads to the hypomethylation of p16. Our results indicate that serine metabolism is involved in stem cell aging by regulating DNA methylation.

## Materials and Methods

### Antibodies

The antibodies to anti-PSAT1 and anti-PHGDH were purchased from Proteintech. The antibodies to anti-DNMT1, DNMT3a, p16, PCNA, and DNMT3b were purchased from Abcam. Anti- $\beta$ -actin antibody was purchased from Sigma-Aldrich. Anti-Ki67-PE antibody was purchased from eBioscience.

### Dental Pulp and DPSC Isolation

The dental pulp of intact human teeth (incisors and premolars) was collected from 3 groups of individuals: deciduous teeth from 5 donors aged 8 to 10 y (mean age, 8.6 y), permanent teeth from 5 donors aged 18 to 21 y (mean age, 19.4 y), and permanent teeth from 5 donors aged 55 to 61 y (mean age, 57.6 y). Each group had 3 females and 2 males. The teeth were extracted for valid clinical reasons (i.e., retained deciduous teeth, orthodontic treatment, or periodontal disease malocclusion). Half of the pulp tissue was used for histologic analysis and the other half was used to isolate DPSCs, as we previously described (Cui et al. 2020). Passages 5 to 8 of DPSCs were used for the functional and pathway analysis. Protocols and procedures

were approved by the Ethical Guidelines of Peking University, and informed consent was obtained from the participants (PKUSSIRB-2013 11103).

### Methylated DNA Immunoprecipitation–Quantitative Polymerase Chain Reaction

Methylated DNA immunoprecipitation–quantitative polymerase chain reaction (MeDIP-qPCR) was performed with the MeDIP Assay Kit (Active Motif) in accordance with the manufacturer's instruction. Briefly, genomic DNA was extracted from SHED, Y-DPSCs, and A-DPSCs and fragmented by sonicating on ice for 10 pulses of 20 s with a 30-s pause on ice between each pulse (30% amplitude). The immunoprecipitation reaction was established with 200 ng of fragmented DNA. The samples were incubated in a polymerase chain reaction machine at 95 °C for 10 min to denature the DNA by following the manufacturer's instruction; then, the magnetic beads and 5-mC antibody with mouse IgG were added as the negative controls. The samples were incubated overnight with end-to-end rotation at 4 °C. The DNA was washed with the buffer provided in the kit and enriched with a magnetic stand. Then, the DNA was used to perform qPCR and to analyze the 5-mC enrichment on the promoter of *p16*. The primers are listed in Appendix Table 1.

### RNA Sequencing and Bioinformatics Analysis

RNA sequencing analysis of total RNA from SHED, Y-DPSCs, and A-DPSCs was performed at the Department of Biotechnology, Beijing Institute of Radiation Medicine. Three RNA samples from each group were used for the RNA sequencing analysis. The sequencing and the analysis were performed as previously described (Yang et al. 2018). The RNA sequencing reads were mapped on the human genome (GRCh38/hg38). Gene Pattern and WebGestalt were used for functional analysis.

### Population Doubling Analysis

The stem cells from serial passages p3, p5, p7, and p9 ( $5 \times 10^5$  cells) were seeded into a 100-mm dish with culture medium to analyze the population doubling (PD) of SHED, Y-DPSCs, and A-DPSCs. The cells were harvested and counted after 3 d. The number of DPSCs at the seeding and harvesting times were determined to calculate the PD per the following formula:  $PD = \frac{\ln(N_f/N_i)}{\ln 2}$ , where  $N_i$  is the initial cell number and  $N_f$  is the harvest cell number (Vidal et al. 2006; Kim et al. 2019).

### Masson Trichrome Staining

The dental pulp tissue sections were stained with modified Masson trichrome staining kits (Solarbio Life Science) in accordance with the manufacturer's instructions. One field of view from the coronal dental pulp near the dentin was randomly selected from each specimen ( $n = 5$ ) for semiquantitative

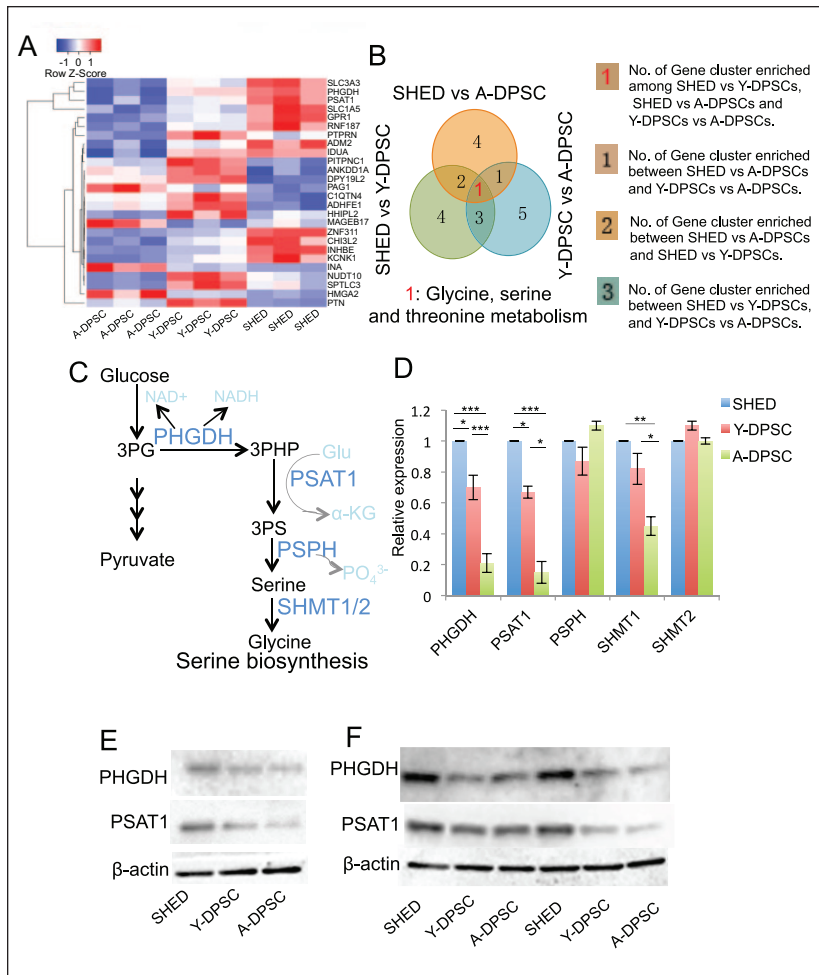


**Figure 1.** Serine biosynthesis proliferates in DPSCs. **(A)** Different gene expression among SHED, Y-DPSCs, and A-DPSCs ( $P < 0.05$  and fold change  $> 2$ ). **(B)** Top 10 gene cluster enrichment between SHED and Y-DPSCs, SHED and A-DPSCs, and Y-DPSCs and A-DPSCs by using KEGG analysis through WebGestalt. 4, 5: number of gene clusters enriched between SHED and Y-DPSCs, SHED and A-DPSCs, and Y-DPSCs and A-DPSCs, respectively. **(C)** The schema for serine biosynthesis. **(D)** Expression of serine metabolism-related genes *PHGDH*, *PSAT1*, *PSPH*, *SHMT1*, and *SHMT2* in SHED, DPSCs, and A-DPSCs, as analyzed with qPCR ( $n = 3$ ). **(E, F)** Expression level of *PHGDH* and *PSAT1* in SHED, Y-DPSCs, and A-DPSCs, as assessed with Western blot. **(A, D)** Statistics were analyzed by analysis of variance with the Bonferroni correction. Values are presented as mean  $\pm$  SD. \* $P < 0.05$ . \*\* $P < 0.01$ . \*\*\* $P < 0.001$ . A-DPSCs, dental pulp stem cells from old adults; DPSCs, dental pulp stem cells; KEGG, Kyoto Encyclopedia of Genes and Genomes; *PHGDH*, phosphoglycerate; *PSAT1*, phosphoserine aminotransferase 1; *PSPH*, phosphoserine phosphatase; qPCR, quantitative polymerase chain reaction; SHED, stem cells from human exfoliated deciduous teeth; *SHMT1* and *SHMT2*, hydroxymethyltransferases 1 and 2; Y-DPSCs, dental pulp stem cells from young adults.

analysis of the collagen/matrix content (Hirate et al. 2012). The positive staining of the collagen/matrix in the dental pulp was analyzed with Image-Pro Plus 6.0 (Media Cybernetics) through integral optical density per area.

### Western Blotting

Total protein was lysed with the M-PER mammalian protein extraction reagent and quantified with the protein concentration assay. Proteins (10  $\mu$ g) were loaded for Western blot as previously described (Yu, Liu, et al. 2019).

### Real-time Polymerase Chain Reaction

Total RNA was extracted from the cultured cells with Trizol (Invitrogen). The SuperScript III Reverse Transcriptase Kit (Invitrogen) was used to synthesize the cDNA to analyze the expression of mRNA. qPCR was performed with the specific primer (Appendix Table 1).

### Methods Described in Detail in the Appendix

Osteogenic differentiation assay  
Adipogenic differentiation assay  
Immunofluorescent staining  
Amino acid analysis  
SAM quantification assay

### Statistics

Data were presented as mean and standard deviation. Comparisons between 2 groups were analyzed with independent unpaired 2-tailed Student *t* tests, and comparisons among  $> 2$  groups were analyzed with 1-way analysis of variance, with Bonferroni correction if the data did not meet the normality distribution assumption by SPSS 19.0 (IBM).  $P < 0.05$  was considered statistically significant.

### Results

#### Expression of Serine Metabolism-Related Genes Decreased in A-DPSCs

We performed the RNA sequencing analysis of DPSCs isolated from the deciduous teeth (SHED) and permanent teeth of young (Y-DPSCs) and old (A-DPSCs) individuals to analyze the gene expression differences among these 3 types of stem cells. Results

showed that the expression levels of 26 genes were the most significantly different among these 3 types of DPSCs (Fig. 1A). The KEGG pathway analysis by WebGestalt among SHED versus Y-DPSCs, SHED versus A-DPSCs, and Y-DPSCs versus A-DPSCs was used to obtain the most enriched 10 gene clusters. Interestingly, glycine, serine, and threonine metabolism was the only gene cluster that could be distinguished in the comparison analysis (Fig. 1B, Appendix Table 2). We then analyzed the expression of serine pathway-related enzymes (*PHGDH*, *PSAT1*, *PSPH*, and *SHMT1/2*). The expression levels of *PHGDH*, *PSAT1*, and *SHMT1* decreased in DPSCs in an

age-dependent manner, as assessed by qPCR (Fig. 1C, D). In addition, the expression of PGHGD and PSAT1 decreased with aging, as verified by Western blot analysis (Fig. 1E, F). Results indicated that serine metabolism decreased in aging DPSCs.

### Stemness of A-DPSCs Decreased as Compared with Y-DPSCs and SHED

We compared the proliferation capacity of SHED, Y-DPSCs, and A-DPSCs by using the BrdU labeling assay and Ki-67 staining by flow cytometry. Results showed that the proliferation rate of A-DPSCs was lower than that of SHED and Y-DPSCs and that the proliferation rate of Y-DPSCs was lower than that of SHED (Fig. 2A, B). The population doubling analysis showed that A-DPSCs became less proliferative from approximately p5 and then ceased growth by approximately p9, whereas Y-DPSCs became less proliferative as compared with SHED from p7 (Appendix Fig. 1). The alizarin red staining showed that the osteogenic differentiation capacity of DPSCs decreased in an age-dependent manner (Fig. 2C), accompanied with the decreased expression of odonto-/osteogenic differentiation-related genes *DSPP*, *RUNX2*, and *OCN*, as assessed by qPCR (Fig. 2D). However, the adipogenic differentiation capacity of A-DPSCs was slightly higher than that of SHED and Y-DPSCs, which was accompanied by the increased expression of adipogenic differentiation-related genes *LPL* and *PPAR $\gamma$*  and indicated that the adipogenic activity increased with aging (Fig. 2E, F). These results showed that the proliferation and osteogenic differentiation capacity of DPSCs decreased with aging.

### Level of Serine Metabolism-Related Genes Decreased in Aging Dental Pulp

We then analyzed the expression of the aging marker p16 (CDNK2A) by using qPCR and Western blot. Results showed that the level of p16 in A-DPSCs was higher than that in Y-DPSCs and SHED (Fig. 3A–C). Then, we collected the dental pulp from deciduous teeth and young and old permanent teeth. The hematoxylin-eosin staining and Masson trichrome staining showed that the dental pulp from old permanent teeth contained more abundant collagen/matrix as compared with

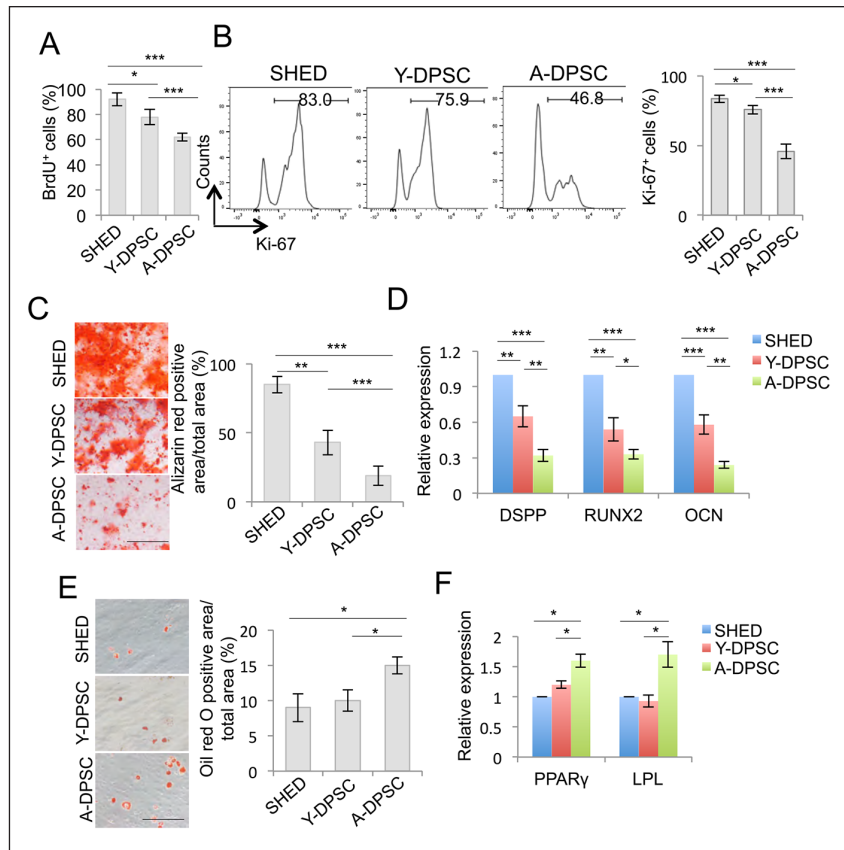


**Figure 2.** A-DPSCs show decreased proliferation and osteogenic differentiation capacity. **(A)** Proliferation of SHED, Y-DPSCs, and A-DPSCs, as assessed with the BrdU labeling assay ( $n = 3$ ). **(B)** Ratio of Ki-67<sup>+</sup> cells in SHED, Y-DPSCs, and A-DPSCs, as assessed with flow cytometry ( $n = 3$ ). **(C)** Odonto-/osteogenic differentiation of SHED, Y-DPSCs, and A-DPSCs, as analyzed with alizarin red staining ( $n = 3$ ). **(D)** Expression of odonto-/osteogenic differentiation-related genes *DSPP*, *RUNX2*, and *OCN*, as analyzed by qPCR ( $n = 3$ ). **(E)** Adipogenic differentiation of SHED, Y-DPSCs, and A-DPSCs, as analyzed with oil red O staining ( $n = 3$ ). **(F)** Expression of adipogenic differentiation-related genes *LPL* and *PPAR $\gamma$*  in SHED, Y-DPSCs, and A-DPSCs, as analyzed with qPCR ( $n = 3$ ). Scale bar (C, E) = 50  $\mu$ m. Statistics were analyzed by analysis of variance. Values are presented as mean  $\pm$  SD. \* $P < 0.05$ . \*\* $P < 0.01$ . \*\*\* $P < 0.001$ . A-DPSCs, dental pulp stem cells from old adults; qPCR, quantitative polymerase chain reaction; SHED, stem cells from human exfoliated deciduous teeth; Y-DPSCs, dental pulp stem cells from young adults.

that from deciduous teeth and young permanent teeth (Fig. 3D, Appendix Fig. 2). Moreover, the ratios of PSAT1- or PHGDH-positive cells in the dental pulp from old permanent teeth were significantly less than those in the dental pulp from deciduous teeth and young permanent teeth (Fig. 3E, F). The ratio of PCNA-positive cells in dental pulp also decreased with aging, which was consistent with the proliferation rate decrease in DPSCs (Fig. 3G). These results indicated that the serine metabolism decreased in aging dental pulp.

### Serine Metabolism Regulated the DNA Methylation of p16 in DPSCs

We analyzed the one-carbon pathway-related amino acid in DPSCs to explore how serine metabolism regulated the capacity of stem cells during aging. Results showed that the level of

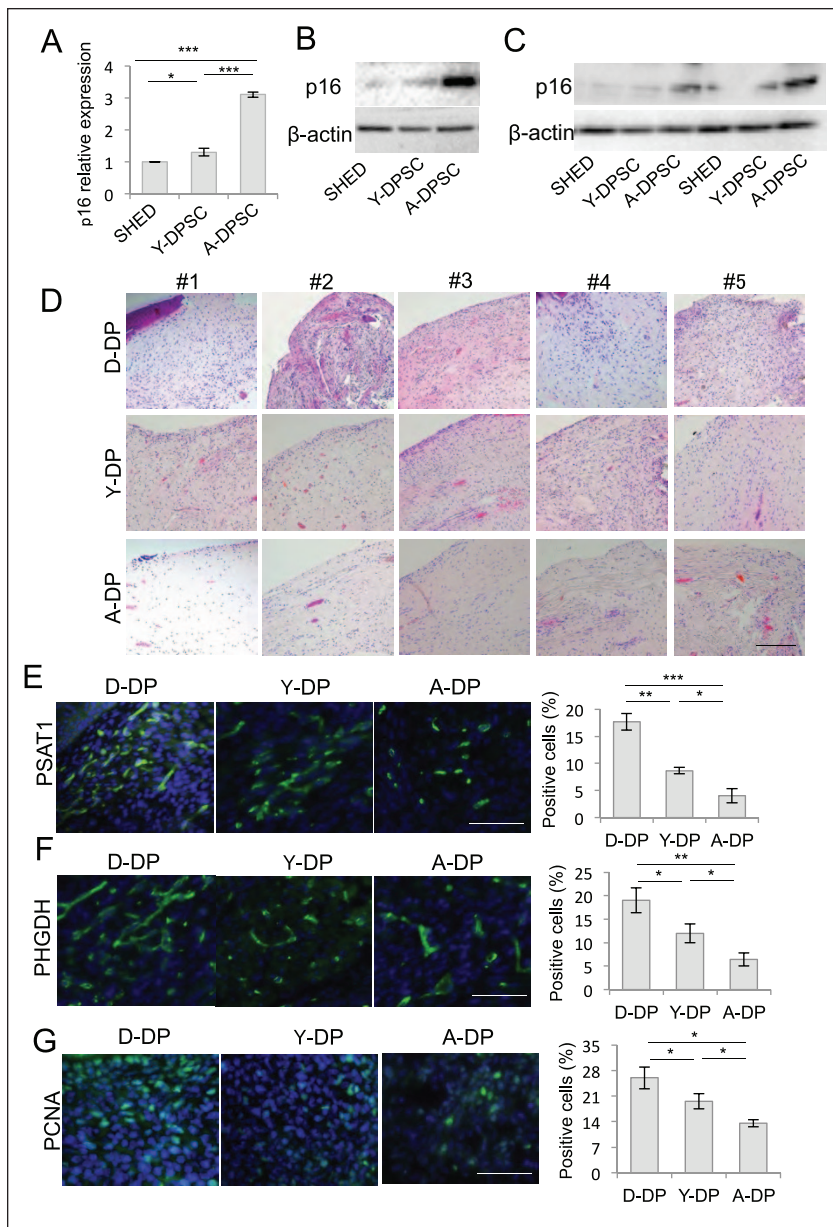


**Figure 3.** Serine metabolism–related genes decreased in aging dental pulp. (A–C) Expression of *p16* in SHED, Y-DPSCs, and A-DPSCs, as analyzed with qPCR ( $n = 3$ ) and Western blot. (D) Histologic structure of the coronal part of dental pulp near the dentin from deciduous teeth ( $n = 5$ ) and young ( $n = 5$ ) and old ( $n = 5$ ) permanent teeth. (E–G) PSAT1-, PHGDH-, or PCNA-positive cells in the dental pulp of deciduous teeth ( $n = 5$ ) and young ( $n = 5$ ) and old ( $n = 5$ ) permanent teeth, as assessed with immunofluorescent staining ( $n = 5$ ). (A, E, F) Statistics was analyzed by analysis of variance. Scale bar (D) = 100  $\mu$ m, (E–G) 25  $\mu$ m. Values are presented as mean  $\pm$  SD. \* $P < 0.05$ . \*\* $P < 0.01$ . \*\*\* $P < 0.001$ . A-DP, dental pulp of aging permanent teeth; A-DPSCs, dental pulp stem cells from old adults; D-DP, dental pulp of deciduous teeth; PCNA, proliferating cell nuclear antigen; PHGDH, phosphoglycerate; qPCR, quantitative polymerase chain reaction; SHED, stem cells from human exfoliated deciduous teeth; Y-DP, dental pulp of young permanent teeth; Y-DPSCs, dental pulp stem cells from young adults.

glycine, serine, and methionine decreased with aging in DPSCs (Fig. 4A–C), suggesting that the intracellular pool of serine, glycine, and methionine decreased in A-DPSCs. Moreover, the

intracellular SAM in A-DPSCs decreased as compared with SHED and Y-DPSCs (Fig. 4D). Then, we wondered whether the DNA methylation of *p16* was different among these 3 DPSCs. Results showed that the 5-mC enrichment levels in CpG1, CpG2, and CpG3 of the *p16* promoter in A-DPSCs was significantly lower than in Y-DPSCs and SHED. The 5-mC enrichment levels in CpG4 in A-DPSCs and SHED. The 5-mC enrichment levels in CpG1, CpG2, and CpG3 of the *p16* promoter in Y-DPSCs were also lower than those in SHED (Fig. 4E, F). Next, we analyzed the expression of DNMT in DPSCs by using qPCR and found that the expression levels of the *DNMT1* and *DNMT3a* in A-DPSCs were lower than those in Y-DPSCs and SHED. The expression level of *DNMT1* was lower in Y-DPSCs than in SHED (Fig. 4G). The expression of *p16* was increased after DNMT1 siRNA treatment in Y-DPSCs and SHED (Fig. 4H; Appendix Fig. 3A, B). These results indicated that the decreased serine metabolism in A-DPSCs reduced the DNA methylation of *p16*, which mediated the cell senescence of A-DPSC.

### PHGDH Regulated the Property of DPSCs via DNA Methylation

To verify the role of serine metabolism on the property of DPSCs and DNA methylation, we knocked down PHGDH with siRNA in SHED and Y-DPSCs and found that the level of SAM decreased after knockdown of PHGDH (Fig. 5A; Appendix Fig. 4A, B). Furthermore, the methylation level on the promoter of *p16* decreased after the knockdown of PHGDH (Fig. 5B; Appendix Fig. 4C), which upregulated the expression of *p16* in SHED and Y-DPSCs (Fig. 5C; Appendix Fig. 4D). The proliferation rate and osteogenic differentiation capacity of SHED and Y-DPSCs decreased after PHGDH siRNA treatment (Fig. 5D, E; Appendix Fig. 4E, F). These results indicated that the serine metabolism decreased in DPSCs in an age-dependent

manner, which supplied less methyl donor to reduce the DNA methylation of *p16* and resulted in the decrease of the property of DPSCs (Fig. 5F).

## Discussion

Aging is linked to the decline of the self-renewal and regenerative capacity of stem cells. In the clinic, pulp capping uses protective materials to expose vital pulp and induce the protective dentin-like layer. The success rate of the pulp capping is significantly lower in older groups (Cho et al. 2013; Marques et al. 2015), which may be related to the declined property of DPSCs. Thus, understanding the characteristic of DPSCs with aging and the underlying molecular mechanisms may allow the improvement of the therapeutic effects of stem cells. Here, we have studied the characteristics of DPSCs isolated from diverse age groups and shown that all 3 groups of DPSCs have the potential to differentiate into osteo-/odontogenic and adipogenic lineages. The proliferation rate and osteogenic differentiation capacity of DPSCs decline with aging. The adipogenic differentiation capacity of A-DPSCs is slightly increased as compared with SHED and Y-DPSCs, whereas no significant difference is observed between SHED and Y-DPSCs. Moreover, we observed the increased expression of aging-related marker p16 in A-DPSCs as compared with SHED and Y-DPSCs. One-carbon metabolism is reported to regulate cell proliferation in cancer development and progression, which provides new therapy targets for tumors (Kottakis et al. 2016; Luengo et al. 2017). One-carbon metabolism is also crucial for T-cell activation and macrophage polarization (Ron-Harel et al. 2016; Yu, Wang, et al. 2019). Macrin et al. (2019) recently reported that the metabolism capacity of DPSCs to utilize fatty acids and glucose may be an early predictor of DPSC aging. Here we have identified that serine metabolism is the most enriched gene cluster among SHED, Y-DPSCs, and A-DPSCs through RNA sequencing analysis. In particular, we have shown that the expression level of serine synthesis genes PHGDH and PSAT1 in A-DPSCs is significantly lower as compared with SHED and Y-DPSCs. The ratios of PHGDH- or PSAT1-positive cells in the old dental pulp are significantly less than those in the dental pulp of deciduous teeth and young permanent teeth. Furthermore, we have detected that the levels of serine, glycine, and methionine are significantly lower than in A-DPSCs, indicating that serine metabolism diminishes with aging. Moreover, the inhibition of PHGDH, the first step in de novo serine synthesis, has down-regulated the proliferation and osteogenic differentiation of

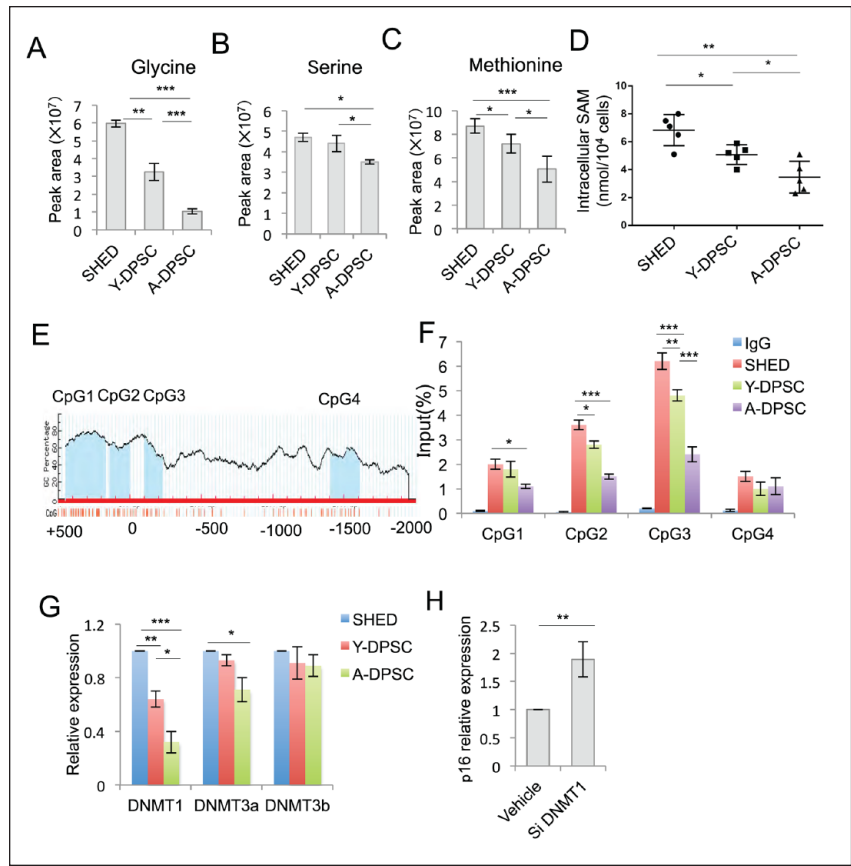


**Figure 4.** Regulation of *p16* methylation by serine metabolism. Mass isotopomer analysis shows the distribution of (A) glycine, (B) serine, and (C) methionine in SHED, Y-DPSCs, and A-DPSCs ( $n = 3$ ). (D) Level of SAM in SHED, Y-DPSCs, and A-DPSCs, as assessed with the SAM quantification assay ( $n = 5$ ). (E) CpG islands on the promoter of *p16* as shown by the meth primer. (F) 5-mC enrichment on the promoter of *p16* in SHED, Y-DPSCs, and A-DPSCs, as analyzed with MeDIP-qPCR ( $n = 3$ ). (G) Expression levels of *DNMT1*, *DNMT3a*, and *DNMT3b* in SHED, Y-DPSCs, and A-DPSCs, as analyzed with qPCR ( $n = 3$ ). (H) Expression of *p16* in the vehicle and DNMT1 siRNA treatment groups of Y-DPSCs ( $n = 3$ ). (A–D, F, G) Statistics were analyzed by analysis of variance and (H) *t* test. Values are presented as mean  $\pm$  SD. \* $P < 0.05$ . \*\* $P < 0.01$ . \*\*\* $P < 0.001$ . A-DPSCs, dental pulp stem cells from old adults; DNMT, DNA methyltransferase; MeDIP-qPCR, methylated DNA immunoprecipitation–quantitative polymerase chain reaction; SAM, S-adenosylmethionine; SHED, stem cells from human exfoliated deciduous teeth; Y-DPSCs, dental pulp stem cells from young adults.

SHED. At least to our knowledge, this study is the first to report that serine metabolism regulates DPSCs and mesenchymal stem cell aging. The one-carbon metabolism supports SAM and histone methylation to drive the macrophage-mediated inflammation (Yu, Wang, et al. 2019), which indicates that the one-carbon metabolism may participate in the inflammation of caries or other oral diseases.

The one-carbon metabolism is a sophisticated network that has several pathways to generate one-carbon units, including the glycine cleavage system, serine metabolism to glycine, and the metabolism of other amino acids and choline (Yang and Vousden 2016). The low dose of N-acetyl-L-cysteine can protect SHED against oxidative damage during the in vitro cultivation toward increasing polyunsaturated fatty acid. L-cysteine promotes the proliferation and differentiation of neural stem

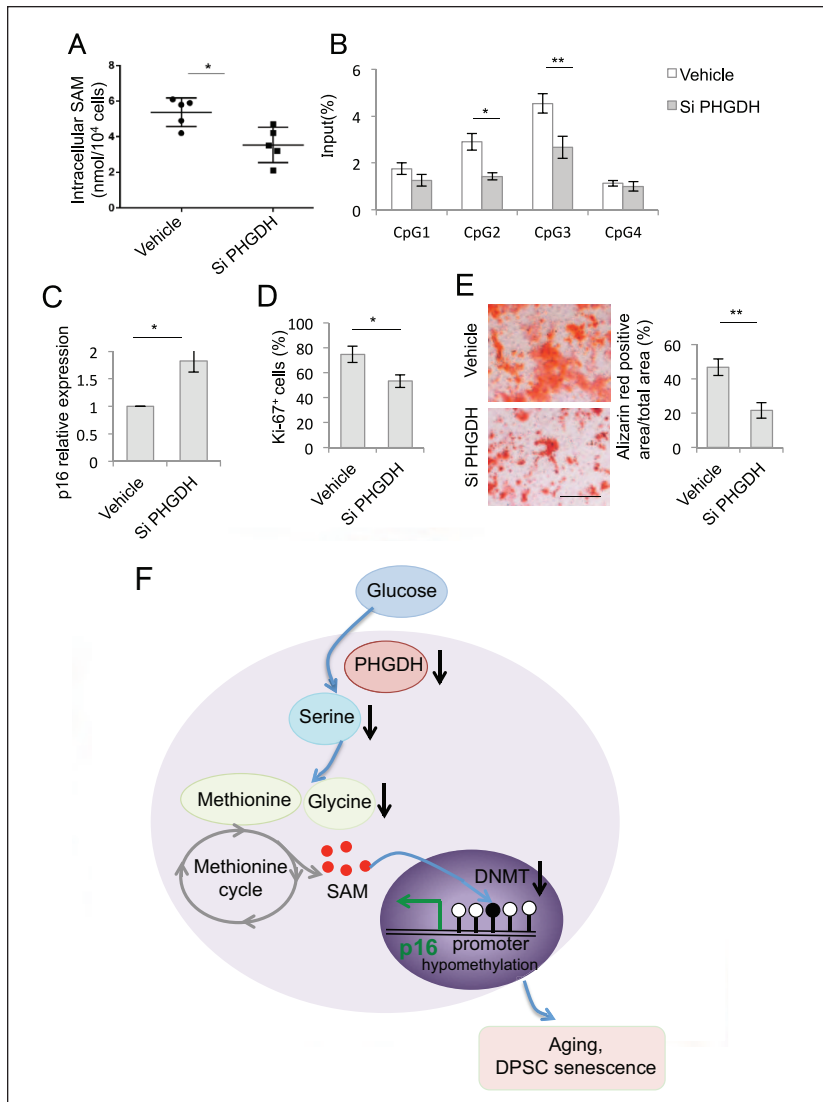


**Figure 5.** Knockdown of PHGDH decreased the stemness of Y-DPSCs. **(A)** Level of SAM in the vehicle and PHGDH siRNA treatment groups of Y-DPSCs ( $n = 5$ ). **(B)** 5-mC enrichment on the promoter of *p16* in the vehicle and PHGDH siRNA treatment groups of Y-DPSCs, as analyzed with MeDIP-qPCR ( $n = 3$ ). **(C)** Expression of *p16* in the vehicle- and siPHGDH-treated Y-DPSCs, as analyzed with qPCR ( $n = 3$ ). **(D)** The ratio of Ki-67<sup>+</sup> cells in the vehicle- and PHGDH siRNA-treated Y-DPSCs, as analyzed with flow cytometry ( $n = 3$ ). **(E)** Osteogenic differentiation of Y-DPSCs in the vehicle and PHGDH siRNA treatment groups ( $n = 3$ ). **(F)** Schematic shows that serine metabolism regulates DPSC aging via the DNA methylation of *p16*. The black arrow indicates that the level of genes decrease with age. Empty dots indicate unmethylated CpGs, and black dots indicate methylated CpGs. Scale bar (F) = 50  $\mu\text{m}$ . (A–E) *t* test. Values are presented as mean  $\pm$  SD. \* $P < 0.05$ . \*\* $P < 0.01$ . DPSC, dental pulp stem cell; MeDIP-qPCR, methylated DNA immunoprecipitation–quantitative polymerase chain reaction; PHGDH, phosphoglycerate; SAM, S-adenosylmethionine; Y-DPSCs, dental pulp stem cells from young adults.

cells via the CBS/H<sub>2</sub>S pathway (Debeljak Martacic et al. 2016; Martacic et al. 2018). Thus, the exact pathway that regulates DPSC aging needs further investigation. Although dentin is a metabolically inactive tissue, posttranslational modifications accumulate with aging in this tissue. Notably, the aspartic acid racemization proceeds at high rates in human dentin, and the

rate of aspartic acid racemization in dentin phosphoproteins and phosphoserine (Ser[P]) contents decreases in dentin with age, which may be related with the deceased level of serine in dental pulp with age (Ohtani and Yamamoto 1992; Cloos and Jensen 2000). Their turnover rate, the nearby specific niche, and the frequency at which they are mobilized shape the metabolic profile of stem cells. Thus, work needs to be done to illustrate the profile of amino acid metabolism in DPSCs, dentin, and their exact function.

DNA methylation is correlated with aging. The inhibition of DNA methyltransferases is reported to induce senescence in mesenchymal stem cells by dysregulating the DNA methylation and promoting the histone modification (Hernando-Herraez et al. 2019; Serefidou et al. 2019). In this study, we have found that A-DPSCs produce less SAM, which is synthesized from threonine catabolism and can provide a methyl donor for DNA and protein methylation (Yang et al. 2018). The decreased level of SAM in A-DPSCs induces the hypomethylation of *p16* in A-DPSCs to elevate its expression. Other genes related to cell aging, such as p53, may be altered by DNA methylation during aging, and this speculation needs further study (Liu et al. 2018). In addition, the level of SAM is downregulated in SHED after the knockdown of PHGDH, resulting in the hypomethylation of *p16* to elevate its expression in SHED. SAM can also provide a methyl donor for histone modification (Serefidou et al. 2019), and whether the histone modification participates in DPSC aging needs additional investigation.

In conclusion, we have identified that serine-dependent one-carbon metabolism contributes to DPSC aging by providing less methyl donor to DNA methylation, resulting in the hypomethylation of *p16* and the increased expression of *p16* in A-DPSCs. This study provides an alternative novel predictor of aging and targets the amelioration of aging-associated phenotypes.

### Author Contributions

R.L. Yang, contributed to conception, design, data acquisition, analysis, and interpretation, drafted and critically revised the manuscript; H.M. Huang, contributed to conception, design, data acquisition, analysis, and interpretation, critically revised the

manuscript; C.S. Han, S.J. Cui, Y.K. Zhou, contributed to data acquisition and analysis, critically revised the manuscript; Y.H. Zhou, contributed to conception, critically revised the manuscript. All authors gave final approval and agree to be accountable for all aspects of the work.

## Acknowledgments

This work was supported by the National Natural Science Foundation of China (Nos. 81970940 and 81600865 to R.L.Y.), the Beijing Natural Science Foundation (No. 7182182 to R.L.Y.), and the National Science and Technology Major Project of the Ministry of Science and Technology of China (No. 2018ZX10302207). The authors declare no potential conflicts of interest with respect to the authorship and/or publication of this article.

## References

- Alt EU, Senst C, Murthy SN, Slakey DP, Dupin CL, Chaffin AE, Kadowitz PJ, Izadpanah R. 2012. Aging alters tissue resident mesenchymal stem cell properties. *Stem Cell Res.* 8(2):215–225.
- Cho SY, Seo DG, Lee SJ, Lee J, Lee SJ, Jung IY. 2013. Prognostic factors for clinical outcomes according to time after direct pulp capping. *J Endod.* 39(3):327–331.
- Cloos PA, Jensen AL. 2000. Age-related de-phosphorylation of proteins in dentin: a biological tool for assessment of protein age. *Biogerontology.* 1(4):341–356.
- Cui SJ, Zhang T, Fu Y, Liu Y, Gan YH, Zhou YH, Yang RL, Wang XD. 2020. DPSCs attenuate experimental progressive TMJ arthritis by inhibiting the STAT1 pathway. *J Dent Res.* 99(4):446–455.
- Debeljak Martacic J, Borozan S, Radovanovic A, Popadic D, Mojsilovic S, Vucic V, Todorovic V, Kovacevic Filipovic M. 2016. N-acetyl-L-cysteine enhances ex-vivo amplification of deciduous teeth dental pulp stem cells. *Arch Oral Biol.* 70:32–38.
- Etcheagaray JP, Mostoslavsky R. 2016. Interplay between metabolism and epigenetics: a nuclear adaptation to environmental changes. *Mol Cell.* 62(5):695–711.
- Fawal MA, Jungas T, Kischel A, Audouard C, Iacovoni JS, Davy A. 2018. Cross talk between one-carbon metabolism, Eph signaling, and histone methylation promotes neural stem cell differentiation. *Cell Rep.* 23(10):2864–2873.e7.
- Gronthos S, Mankani M, Brahimi J, Robey PG, Shi S. 2000. Postnatal human dental pulp stem cells (DPSCs) in vitro and in vivo. *Proc Natl Acad Sci U S A.* 97(25):13625–13630.
- Hernando-Herraez I, Evano B, Stubbs T, Commere PH, Jan Bonder M, Clark S, Andrews S, Tajbakhsh S, Reik W. 2019. Ageing affects DNA methylation drift and transcriptional cell-to-cell variability in mouse muscle stem cells. *Nat Commun.* 10(1):4361.
- Hirate Y, Yamaguchi M, Kasai K. 2012. Effects of relaxin on relapse and periodontal tissue remodeling after experimental tooth movement in rats. *Connect Tissue Res.* 53(3):207–219.
- Kim C, Park JM, Song Y, Kim S, Moon J. 2019. HIF1 $\alpha$ -mediated AIMP3 suppression delays stem cell aging via the induction of autophagy. *Aging Cell.* 18(2):e12909.
- Kottakis F, Nicolay BN, Roumane A, Karnik R, Gu H, Nagle JM, Boukhali M, Hayward MC, Li YY, Chen T, et al. 2016. LKB1 loss links serine metabolism to DNA methylation and tumorigenesis. *Nature.* 539(7629):390–395.
- Kurniawan H, Franchina DG, Guerra L, Bonetti L, Bagnuet LS, Grusdat M, Schlicker L, Hunewald O, Dostert C, Merz MP, et al. 2020. Glutathione restricts serine metabolism to preserve regulatory T cell function. *Cell Metab.* 31(5):920–936.e7.
- Liu W, Zhang L, Xuan K, Hu C, Liu S, Liao L, Li B, Jin F, Shi S, Jin Y. 2018. Alpl prevents bone ageing sensitivity by specifically regulating senescence and differentiation in mesenchymal stem cells. *Bone Res.* 6:27. Erratum in: *Bone Res.* 2020;8:29.
- Locasale JW. 2013. Serine, glycine and one-carbon units: cancer metabolism in full circle. *Nat Rev Cancer.* 13(8):572–583.
- Luengo A, Gui DY, Vander Heiden MG. 2017. Targeting metabolism for cancer therapy. *Cell Chem Biol.* 24(9):1161–1180.
- Macrin D, Alghadeer A, Zhao YT, Miklas JW, Hussein AM, Detraux D, Robitaille AM, Madan A, Moon RT, Wang Y, et al. 2019. Metabolism as an early predictor of DPSCs aging. *Sci Rep.* 9(1):2195.
- Maddocks OD, Labuschagne CF, Adams PD, Vousden KH. 2016. Serine metabolism supports the methionine cycle and DNA/RNA methylation through de novo ATP synthesis in cancer cells. *Mol Cell.* 61(2):210–221.
- Marques MS, Wesselink PR, Shemesh H. 2015. Outcome of direct pulp capping with mineral trioxide aggregate: a prospective study. *J Endod.* 41(7):1026–1031.
- Martacic J, Filipovic MK, Borozan S, Cvetkovic Z, Popovic T, Arsic A, Takic M, Vucic V, Glibetic M. 2018. N-acetyl-L-cysteine protects dental tissue stem cells against oxidative stress in vitro. *Clin Oral Investig.* 22(8):2897–2903.
- Mentch SJ, Mehrmohamadi M, Huang L, Liu X, Gupta D, Mattocks D, Gomez Padilla P, Ables G, Bamman MM, Thalacker-Mercer AE, et al. 2015. Histone methylation dynamics and gene regulation occur through the sensing of one-carbon metabolism. *Cell Metab.* 22(5):861–873.
- Miura M, Gronthos S, Zhao M, Lu B, Fisher LW, Robey PG, Shi S. 2003. SHED: stem cells from human exfoliated deciduous teeth. *Proc Natl Acad Sci U S A.* 100(10):5807–5812.
- Morszczek C. 2019. Cellular senescence in dental pulp stem cells. *Arch Oral Biol.* 99:150–155.
- Nozu A, Hamano S, Tomokiyo A, Hasegawa D, Sugii H, Yoshida S, Mitarai H, Taniguchi S, Wada N, Maeda H. 2018. Senescence and odontoblastic differentiation of dental pulp cells. *J Cell Physiol.* 234(1):849–859.
- Ohtani S, Yamamoto K. 1992. Estimation of age from a tooth by means of racemization of an amino acid, especially aspartic acid—comparison of enamel and dentin. *J Forensic Sci.* 37(4):1061–1067.
- Ren R, Ocampo A, Liu GH, Izpisua Belmonte JC. 2017. Regulation of stem cell aging by metabolism and epigenetics. *Cell Metab.* 26(3):460–474.
- Rodriguez AE, Ducker GS, Billingham LK, Martinez CA, Mainolfi N, Suri V, Friedman A, Manfredi MG, Weinberg SE, Rabinowitz JD, et al. 2019. Serine metabolism supports macrophage IL-1 $\beta$  production. *Cell Metab.* 29(4):1003–1011.e4.
- Ron-Harel N, Santos D, Ghergurovich JM, Sage PT, Reddy A, Lovitch SB, Dephondre N, Satterstrom FK, Sheffer M, Spinelli JB, et al. 2016. Mitochondrial biogenesis and proteome remodeling promote one-carbon metabolism for T cell activation. *Cell Metab.* 24(1):104–117.
- Serefidou M, Venkatasubramani AV, Imhof A. 2019. The impact of one carbon metabolism on histone methylation. *Front Genet.* 10:764.
- Sharpless NE, DePinho RA. 2007. How stem cells age and why this makes us grow old. *Nat Rev Mol Cell Biol.* 8(9):703–713.
- Tang X, Li W, Wen X, Zhang Z, Chen W, Yao G, Chen H, Wang D, Shi S, Sun L. 2019. Transplantation of dental tissue-derived mesenchymal stem cells ameliorates nephritis in lupus mice. *Ann Transl Med.* 7(7):132.
- Van Winkle LJ, Ryznar R. 2019. One-carbon metabolism regulates embryonic stem cell fate through epigenetic DNA and histone modifications: implications for transgenerational metabolic disorders in adults. *Front Cell Dev Biol.* 7:300.
- Vidal MA, Kilroy GE, Johnson JR, Lopez MJ, Moore RM, Gimble JM. 2006. Cell growth characteristics and differentiation frequency of adherent equine bone marrow-derived mesenchymal stromal cells: adipogenic and osteogenic capacity. *Vet Surg.* 35(7):601–610.
- Xuan K, Li B, Guo H, Sun W, Kou X, He X, Zhang Y, Sun J, Liu A, Liao L, et al. 2018. Deciduous autologous tooth stem cells regenerate dental pulp after implantation into injured teeth. *Sci Transl Med.* 10(455):eaaf3227.
- Yamaza T, Kentaro A, Chen C, Liu Y, Shi Y, Gronthos S, Wang S, Shi S. 2010. Immunomodulatory properties of stem cells from human exfoliated deciduous teeth. *Stem Cell Res Ther.* 1(1):5.
- Yang M, Vousden KH. 2016. Serine and one-carbon metabolism in cancer. *Nat Rev Cancer.* 16(10):650–662.
- Yang R, Yu T, Kou X, Gao X, Chen C, Liu D, Zhou Y, Shi S. 2018. Tet1 and Tet2 maintain mesenchymal stem cell homeostasis via demethylation of the P2rx7 promoter. *Nat Commun.* 9(1):2143.
- Yu T, Liu D, Zhang T, Zhou Y, Shi S, Yang R. 2019. Inhibition of Tet1- and Tet2-mediated DNA demethylation promotes immunomodulation of periodontal ligament stem cells. *Cell Death Dis.* 10(10):780.
- Yu W, Wang Z, Zhang K, Chi Z, Xu T, Jiang D, Chen S, Li W, Yang X, Zhang X, et al. 2019. One-carbon metabolism supports S-adenosylmethionine and histone methylation to drive inflammatory macrophages. *Mol Cell.* 75(6):1147–1160.e5.